

Quantum Hall resistance standard based on graphene grown by chemical vapor deposition on silicon carbide

F. Lafont¹, R. Ribeiro-Palau¹, D. Kazazis², A. Michon³, O. Couturaud⁴, C. Consejo⁴, T. Chassagne⁵, M. Zielinski⁵, M. Portail³, B. Jouault⁴, F. Schopfer¹ and W. Poirier^{1*}

¹*LNE - Laboratoire National de Métrologie et d'Essais, avenue Roger Hennequin, 78197 Trappes, France*

²*LPN - Laboratoire de Photonique et de Nanostructures, CNRS, Route de Nozay, 91460 Marcoussis, France*

³*CRHEA - Centre de Recherche sur l'Hétéroépitaxie et ses Applications, CNRS, rue Bernard Grégory, 06560 Valbonne, France*

⁴*L2C - Laboratoire Charles Coulomb, CNRS-Université de Montpellier II, Place Eugène Bataillon, 34095 Montpellier, France and*

⁵*NOVASiC, Savoie Technolac, Arche Bat 4, 73375 Le Bourget du Lac, France*
(Dated: May 3, 2019)

Replacing GaAs-based quantum Hall resistance standards (QHRS) by more convenient graphene based ones is still an ongoing goal in metrology. Although the required 10^{-9} -precision has been reported in graphene based QHRS, these demonstrations were presented from a unique epitaxial graphene source and under high magnetic fields. A requirement to set graphene-based QHRS is the availability of other sources of graphene allowing the operation at lower magnetic fields. Here, we report on a 10^{-9} -accurate quantized resistance over a 9 T range starting from 10 T on the $\nu = 2$ plateau, at a temperature of 1.4 K, in a large Hall bar QHRS made of graphene grown by chemical vapor deposition (CVD) on SiC. The relative discrepancy between the quantized Hall resistances in the graphene sample and in a reference GaAs one is equal to $(-2 \pm 4) \times 10^{-10}$. Using a current amplifier based on a superconducting quantum interference device to study the low dissipation in the QHE regime, we show that the physics of the Hall resistance plateau is characterized by a localization length of states at Fermi energy locked to the magnetic length over a large magnetic field range. This behavior is correlated with the structural properties of the CVD graphene. These results give a new proof of the universality of the QHE and constitute a further step towards a more convenient QHRS. They also demonstrate that CVD on SiC, a recently developed, hybrid and scalable growth technique, is now mature for applications.

The metrology of the resistance unit has been continuously progressing since the discovery that the transverse resistance of a two-dimensional electron gas (2DEG) in a perpendicular magnetic field is quantized at universal values R_K/i , where $R_K \equiv h/e^2$ is the von Klitzing constant, h the Planck constant, e the electron charge, and i an integer[1]. Currently, using GaAs-based heterostructures to form the 2DEG, it has been possible to develop quantum Hall resistance standards (QHRS) reproducible within some parts in 10^{11} [2], as well as accurate low and high resistance QHRS arrays[3] and QHRS adapted to the alternative current (AC) regime. More recently, it has been considered by metrologists that an accurate QHRS could be developed in graphene[4, 5], possibly surpassing the usual GaAs based ones.

The Dirac physics in monolayer graphene manifests itself by a quantum Hall effect (QHE)[6, 7] with Landau levels (LLs) at energies $\pm v_F \sqrt{2\hbar n e B}$ with a $4eB/h$ degeneracy (valley and spin) and a sequence of Hall resistance plateaus at $R_H = \pm R_K/(4(n + 1/2))$ (with $n \geq 0$) [8]. The energy spacing between the two first LLs, $\Delta E(B) = 36\sqrt{B[\text{T}]} \text{ meV}$, is much larger than in GaAs ($1.7B[\text{T}] \text{ meV}$) for currently accessible magnetic fields. It results that the $R_K/2$ can be observable even at room temperature[9]. This opens the way towards a more convenient QHRS in graphene[4, 10] operating at lower magnetic fields ($B \leq 4 \text{ T}$), higher temperatures ($T \geq 4 \text{ K}$) and higher measurement currents ($I \geq 100 \mu\text{A}$) compared to its GaAs counterpart. From previous measurements of the Hall resistance quantization in graphene produced by various methods (exfoliation of graphite, chemical vapor deposition (CVD) on metal, and silicon (Si) sublimation from silicon carbide (SiC), it was concluded that the production of graphene based QHRS requires large graphene monolayers (few $10000 \mu\text{m}^2$) with homogeneous low carrier densities ($< 2 \times 10^{11} \text{ cm}^{-2}$) and high carrier mobilities ($\geq 5000 \text{ cm}^2 \text{ V}^{-1} \text{ s}^{-1}$). Thus, the exfoliation technique was quickly discarded because it produces few monolayers of rather small size and it lacks reproducibility [5, 11–13]. In the case of graphene grown by CVD on metal and transferred on SiO_2/Si substrate, it was shown that the presence of grain boundaries and wrinkles jeopardizes the quantization[14, 15]. In monolayer graphene grown by Si sublimation on the silicon face of SiC, the quantization of the Hall resistance, on the $\nu = 2$ plateau, has been measured with a relative uncertainty of 9×10^{-11} (1σ) at $B=14 \text{ T}$ and $T=0.3 \text{ K}$ [16, 17]. However, such a precision of 10^{-9} or lower, as required in national metrology institutes, was obtained under experimental conditions that do not surpass the GaAs-based ones and was possible to achieve in a few samples coming from only one source, which compromises the reproducibility of the graphene based QHRS (G-QHRS). The Hall resistance recently measured in samples with

lower carrier densities produced from the same graphene source, and having $\nu = 2$ at magnetic fields ranging from 1 T to 8 T, demonstrated an unsatisfying accuracy from about 10^{-6} to a few 10^{-8} [18].

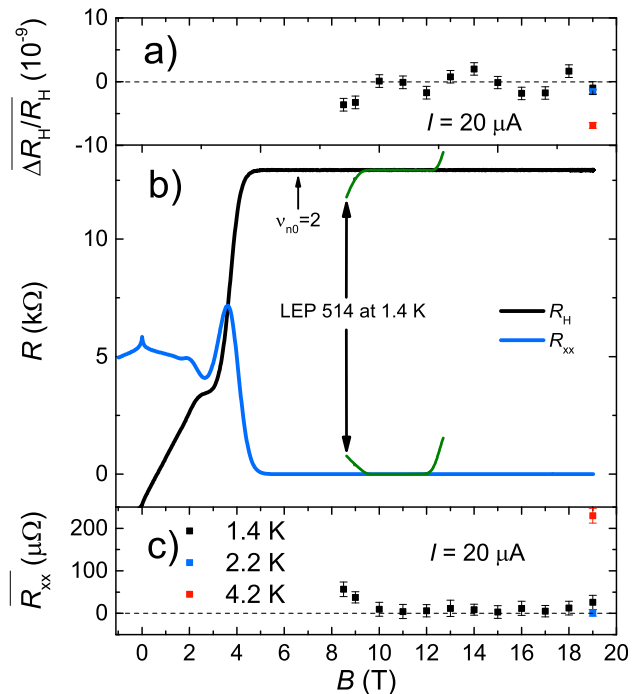


FIG. 1. a) Hall resistance deviation $\overline{\Delta R_H/R_H}$ versus magnetic field B . b) Longitudinal (R_{xx}) and transversal (R_H) resistances (measured with a 100 nA current) as a function of B varying from 0 T to 19 T for the graphene sample (blue curve) and varying from 8 T to 13 T for the GaAs sample (green curve). ν_{n_0} is the Landau level filling factor calculated from the carrier density n_0 determined at low magnetic fields. c) Longitudinal resistance $\overline{R_{xx}}$ versus B . Error bars correspond to one standard deviation (1σ).

Here, we report a 10^{-9} accuracy of the quantum Hall resistance over a 9 T range of magnetic fields from $B=10 \text{ T}$ up to $B=19 \text{ T}$ at a temperature $T=1.4 \text{ K}$ in a G-QHRS made of monolayer graphene grown by propane/hydrogen CVD on SiC[19], a hybrid technique which allows the tuning of the electronic transport properties [20]. These cryomagnetic experimental conditions overlap, for the first time, that of the reference GaAs-based QHRS (GaAs-QHRS) used, making this device an operational QHRS substitute. The discrepancy between the quantized Hall resistance measured in the graphene sample and in the GaAs-based ones is found equal to $(-2 \pm 4) \times 10^{-10}$ (one standard deviation, 1σ), which constitutes a new proof of the universality of the QHE in graphene. The QHE physics of the large $\nu = 2$ ($\nu = \hbar n_S/eB$ is the Landau level filling factor and n_S the carrier density) Hall resistance plateau is investigated using accurate measurement techniques based on specialized metrological instruments. It turns out that the dissipation is dominated by

* wilfrid.poirier@lne.fr.

the variable range hopping (VRH) mechanism. The wide quantized Hall resistance plateau is characterized by a localization length of states at Fermi energy, determined from VRH, that stays very close to the magnetic length over a large magnetic field range of 9 T. This is likely caused by a pinning of the LL filling factor at $\nu = 2$ due to a charge transfer from the donor states in an interface layer between the SiC and the graphene. This work shows that the propane/hydrogen CVD on SiC growth method, which was initiated in 2010[19], is now mature and very promising to develop a challenging G-QHRS surpassing the GaAs-QHRS in the near future.

Results

Magneto-resistance characterizations. Fig. 1-b) shows the Hall resistance R_H and the longitudinal resistance R_{xx} measured as a function of the magnetic field B at a temperature $T=1.4$ K and a measurement current of 100 nA in a large $100 \times 420 \mu\text{m}^2$ Hall bar sample made of graphene grown on the Si face of SiC by propane/hydrogen CVD under a mixture of propane, hydrogen and argon[19, 21] (see Methods). At low magnetic fields, from the Hall slope and the Drude resistivity, a low electron density $n_0 = 3.2 \times 10^{11} \text{cm}^{-2}$ and an electronic mobility $\mu = 3800 \text{cm}^2 \text{V}^{-1} \text{s}^{-1}$ are calculated. Prior to any treatment and Hall bar patterning, the graphene device was initially characterized by a high n-doping (10^{13}cm^{-2}). The low carrier density n_0 was obtained only after annealing the graphene device in vacuum for 1 min at 500°C prior to the Hall bar fabrication and its coating with poly(methylmethacrylate-*co*-methacrylate acid) copolymer P(MMA-MAA) and poly(methylstyrene-*co*-chloromethylacrylate) (ZEP520A). The ZEP520A resist is known to reduce the electron density under UV illumination[22, 23]. Nonetheless, no illumination was done in our case. At higher magnetic fields, a wide and well-quantized $R_K/2$ Hall resistance plateau can be observed, from $B=5$ T up to $B=19$ T (maximum accessible magnetic field in our set-up) and coinciding with a zero minimum of R_{xx} . It extends far beyond the magnetic field $B=6.6$ T at which $\nu_{n0} = 2$, where ν_{n0} is the LL filling factor calculated from the carrier density determined at low magnetic fields. One can also notice the $R_K/6$ Hall resistance plateau between 2 T and 3 T. The comparison is striking when one compares the $R_K/2$ Hall resistance plateau with the one of the most widespread GaAs-based QHR (LEP514[24]) in national metrology institutes which only extends over 2 T starting from 10 T (green curve). Fig. 2 shows the color rendering of the longitudinal resistance R_{xx} per square measured as a function of the measurement current I and of the magnetic field B . It shows that the 2D electron gas is not significantly dissipative ($R_{xx} < 0.25 \text{m}\Omega$) for currents as high as $40 \mu\text{A}$ in the large range of magnetic field between 10 T and 19 T. At a current of $20 \mu\text{A}$,

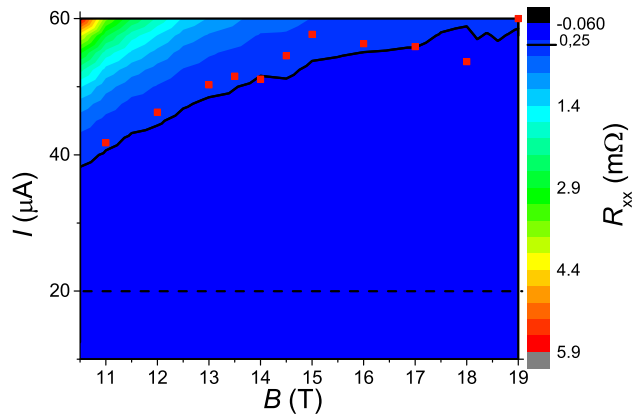


FIG. 2. Color rendering of the longitudinal resistance R_{xx} as a function of the measurement current I and the magnetic field B at $T = 1.4$ K. The $I_C(B)$ black line corresponds to $R_{xx} = 0.25 \text{m}\Omega$. In red dots, better adjustment $\propto \xi(B)^{-2}$ of $I_C(B)$.

lower than the afore mentioned limit, we first carried out three-terminal measurements of contact resistances in the $R_K/2$ Hall plateau. All contacts between metallic pads and graphene, except one (not used), are ohmic with a resistance lower than 1Ω . We then performed accurate four-probes measurements of R_H and R_{xx} using two Hall terminal-pairs ((V1,V4) and (V2,V3)) and two longitudinal terminal-pairs ((V1,V2) and (V3,V5))(see Methods).

Resistance quantization. R_H is indirectly compared with $R_K/2$ given by a reference GaAs-based QHRS (LEP514) using a 100Ω transfer resistor. The comparison is performed using a resistance bridge equipped with a cryogenic current comparator (CCC). To minimize measurement errors of the resistance bridge, the same measurement current is used both in the graphene and the GaAs QHRS. All uncertainties reported in the following are given within one standard deviation (1σ). Let us note $\Delta R_H/R_H$ the relative deviation of the Hall resistance R_H to $R_K/2$ ($\Delta R_H = R_H - R_K/2$). $\Delta R_H/R_H$ and $\overline{R_{xx}}$ are obtained from the mean value of the measurements performed using the two Hall terminal-pairs and the two longitudinal terminal-pairs (on both edges of the Hall bar). Fig. 1-a) reports $\Delta R_H/R_H$ values determined with a standard uncertainty around 1×10^{-9} (the main contribution comes from the instability of the 100Ω transfer resistor) as a function of B for a measurement current of $20 \mu\text{A}$ and a temperature $T=1.4$ K. It shows a perfect quantization of the Hall resistance over the whole magnetic field range of 9 T between $B=10$ T and $B=19$ T, which coincides with $\overline{R_{xx}}$ values lower than $30 \pm 20 \mu\Omega$ (see Fig. 1-c)): all discrepancies of $\Delta R_H/R_H$ to zero are within two standard deviations (2σ corresponding to a coverage factor of 95%). More sensitive measurements performed with the CCC (see Methods) show that $\overline{R_{xx}}$ amounts to $(10.5 \pm 2.4) \mu\Omega$

and $(1.2 \pm 1.7) \mu\Omega$ at $B=10$ T and $B=19$ T respectively, demonstrating a very low dissipation level in the graphene electron gas. Measurements show that the R_H values determined from the two Hall terminal-pairs are in agreement within a relative uncertainty of about 1×10^{-9} , demonstrating the homogeneity of the Hall quantization in the sample over a large surface. The mean value of $\overline{\Delta R_H/R_H}$ measurements carried out at magnetic fields between 10 T and 19 T is $(-2 \pm 4) \times 10^{-10}$. Below $B=9$ T, the Hall resistance starts to deviate from the quantized value and the longitudinal resistance significantly increases. It is remarkable that the G-QHRS can operate accurately at magnetic fields as low as the ones of the reference GaAs-QHRS ($10 \text{ T} \leq B \leq 11 \text{ T}$) with a similar temperature of 1.4 K. This is the first demonstration that a G-QHRS can directly replace a GaAs-QHRS in a conventional QHE setup of a national metrology institute equipped with a 12 T magnet. Fig. 1-a) and c) also report that $\overline{\Delta R_H/R_H}$ is equal to $(-1.5 \pm 0.4) \times 10^{-9}$ and $(-7 \pm 0.5) \times 10^{-9}$ at $T=2.2$ K and $T=4.2$ K respectively. This is due to an increase of $\overline{R_{xx}}$ reaching $0.23 \text{ m}\Omega$ at $T=4.2$ K.

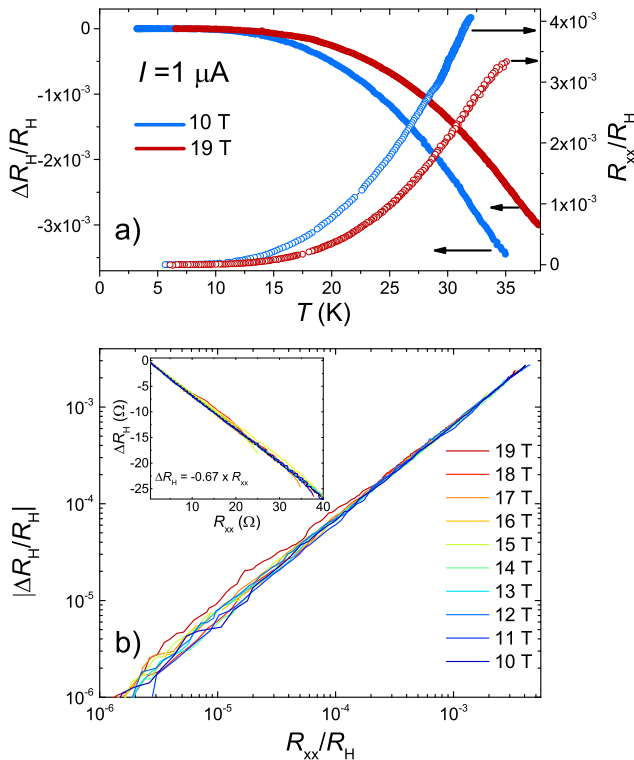


FIG. 3. a) $\Delta R_H/R_H$ (filled circles) and R_{xx}/R_H (empty circles) as a function of the temperature T for two magnetic fields $B=10$ T (blue) and $B=19$ T (red). b) $|\Delta R_H/R_H|$ as a function of R_{xx}/R_H for several magnetic fields B in log-log scale. Inset: ΔR_H as a function of R_{xx} .

The relationship between $R_H(T)$ and $R_{xx}(T)$ was investigated in the range from 3 K to 30 K by performing measurements (using one Hall terminal pair and one lon-

gitudinal terminal pair) at magnetic fields between $B=10$ T and $B=19$ T using a low AC (2 Hz frequency) current of $1 \mu\text{A}$. From measurements of both $R_H(T)$ and $R_{xx}(T)$ (fig. 3-a)), one can report $\Delta R_H/R_H(T)$ as a function of $R_{xx}(T)/R_H(T)$ for several B values in log-log scale (see fig. 3-b)). All curves superpose on a single straight line of unitary slope over four decades of R_{xx} . This corresponds to a relationship $\Delta R_H = -0.67 \times R_{xx}$ (see inset of fig. 3-b)). The same relationship is found by varying the magnetic field at a given temperature (not shown). These linear relationships can be described by an effective geometric coupling between R_H and R_{xx} . In GaAs-based QHR standards, this coupling is usually explained by the finite width of the voltage terminal arms with respect to the Hall bar channel[4, 25] or the inhomogeneous circulation of the current (for example due to the residual inhomogeneity of the carrier density)[26, 27]. The first mechanism would lead to a coupling factor of $(-l/W) = -0.2$, where $l = 20 \mu\text{m}$ is the width of the voltage arm and $W = 100 \mu\text{m}$ is the width of the Hall bar channel. On the other hand, the specific injection of the current by the I_1 terminal or the presence of bilayer patches along SiC steps oriented at 45° with respect to the Hall bar orientation, which represents about 10 % of the total surface in this sample[20] (see Methods) can cause a tilted circulation of the current explaining the observed coupling. We can therefore conclude that a 10^{-9} accuracy of the Hall resistance is typically ensured for an R_{xx} value lower than $15 \mu\Omega$. The longitudinal resistance values of $(10.5 \pm 2.4) \mu\Omega$ and $(1.2 \pm 1.7) \mu\Omega$ measured at $B=10$ T and $B=19$ T should lead to relative discrepancies to $R_K/2$ of 6 parts in 10^{10} and 6 parts in 10^{11} respectively, experimentally not observable in fig. 1.

Dissipation through the variable range hopping mechanism. To better understand the dissipation mechanism that alters the Hall quantization, fig. 4-a) shows $\sigma_{xx}(T) \times T$ plotted in logarithmic scale as a function of $T^{-1/2}$, where $\sigma_{xx} = R_{xx}/(R_{xx}^2 + R_H^2)$ is the longitudinal conductivity. The linearity of the curves over five orders of magnitude allows the description $\sigma_{xx}(T) \times T = \sigma_0(B) \exp[-(T_0(B)/T)^{1/2}]$ where $T_0(B)$ and $\sigma_0(B)$ are B -dependent fitting parameters, as expected from a dissipation mechanism based on variable range hopping with soft Coulomb gap [28]. Thermal activation does not manifest itself in the temperature range investigated, up to 40 K. Fig. 4-b) shows a sub-linear increase of $T_0(B)$ as a function of B with a saturation around 2500 K at the highest magnetic field. If we assume that $k_B T_0(B) = C e^2 / (4\pi \epsilon_r \epsilon_0 \xi(B))$ where $C=6.2$ [29, 30], k_B is the Boltzmann constant, ϵ_0 is the vacuum dielectric constant, $\epsilon_r = (\epsilon_{\text{SiC}} + \epsilon_{\text{P(MMA-MAA)}})/2 = 7.25$ (with $\epsilon_{\text{SiC}} = 10$ [31] and $\epsilon_{\text{P(MMA-MAA)}} = 4.5$ is the value chosen, usually attributed to PMMA alone) is the mean relative dielectric constant of the graphene on SiC covered by the P(MMA-MAA) copolymer, then it is possible to determine the localization length $\xi(B)$ as a function of the magnetic field B . Fig. 4-b) shows that $\xi(B)$ contin-

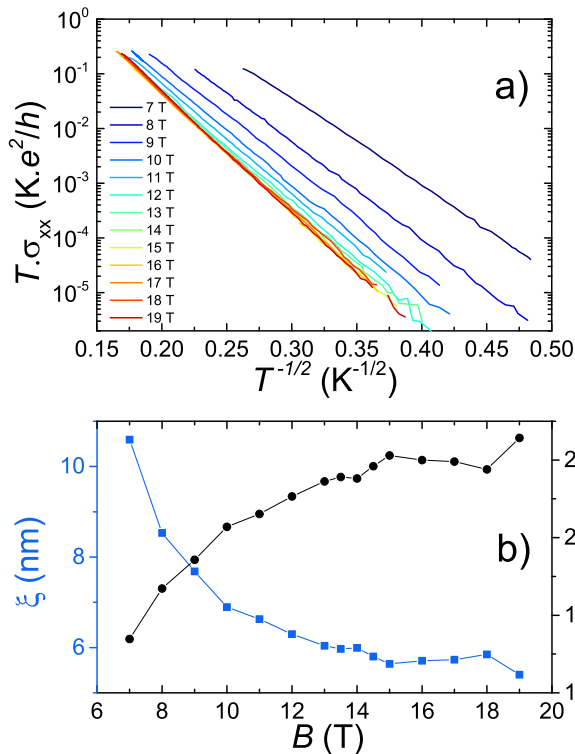


FIG. 4. a) $T\sigma_{xx}$ as a function of $T^{-1/2}$ for several magnetic fields. b) T_0 and ξ versus B .

uously decreases from 10.5 nm to about 5.5 nm between $B=7$ T and $B=19$ T but does not show a minimal value at $B=6.6$ T where $\nu_{n0} = 2$. This continuous decrease of $\xi(B)$ explains the robustness of the Hall resistance plateau towards high magnetic fields.

It is also interesting to know whether the VRH mechanism can explain the dependence of R_{xx} on the current reported in fig. 2 and fig.5-a). The VRH backscattering mechanism predicts that the current I manifests itself as an effective temperature $T_{eff}(I) = eR_H I \xi / (2k_B W)$ [30] where W is the sample width in the hypothesis of a homogenous electric field. It results that $\sigma_{xx} \propto \exp(-I_0/I)^{1/2}$ at $T=0$ K where $I_0 = 2k_B T_0 W / (eR_H \xi)$ is a B -dependent current parameter. For several B values, the effective temperature $T_{eff}(I)$ is determined by matching $\sigma_{xx}(T_{eff}) = \sigma_{xx}(I)$, where $\sigma_{xx}(I)$ is the conductivity measured as a function of the current and $\sigma_{xx}(T) = (\sigma_0/T) \exp[(-T_0/T)^{1/2}]$ was determined previously from the data of fig. 4-a). For all B values, fig. 5b) shows a linear relationship between T_{eff} and I as expected for the VRH mechanism. From the slope of $T_{eff}(I)$ curves and the previous determination of $\xi(B)$, we can therefore extract an effective width $W_{eff} \sim 7.5 \mu\text{m}$, quite independent of the magnetic field, which is much smaller than the Hall bar channel width $W = 100 \mu\text{m}$. This indicates a non-homogeneity of the current flow in the sample, contrary to what has been usually observed in GaAs-based QHRS[32]. We ar-

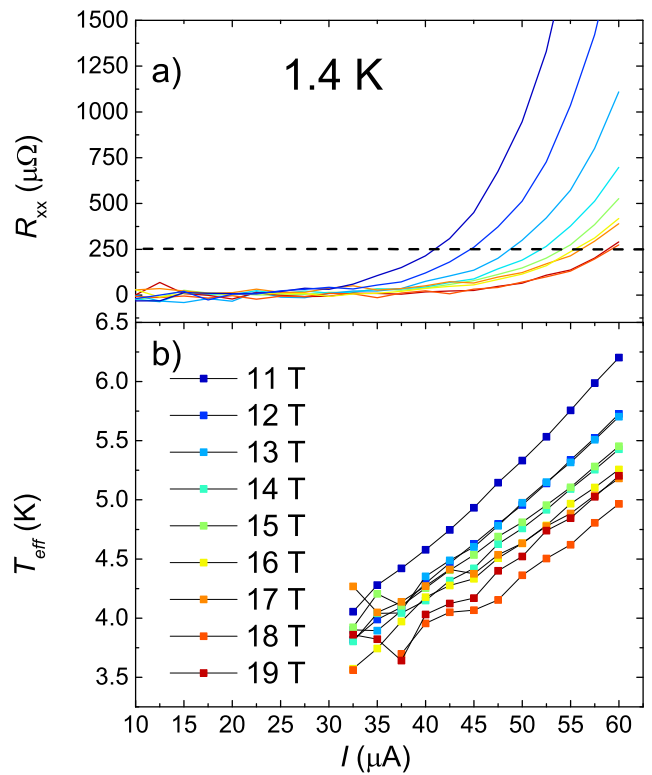


FIG. 5. a) R_{xx} as a function of the current at 1.4 K for different magnetic fields. b) Effective temperature T_{eff} as a function of I (giving $\sigma_{xx}(T_{eff}) = \sigma_{xx}(I)$) for several magnetic fields B . The magnetic field color code is the same for both figures.

gue that the presence of bilayer patches along the SiC edge steps can explain this result. In epitaxial graphene grown by sublimation of SiC[33], it was shown that bilayer stripes are metallic at carrier densities higher than $5 \times 10^{10} \text{cm}^{-2}$. They can drastically alter the Hall quantization if they cross the Hall bar channel by short-circuiting the edge states[33–35]. In our sample, bilayer patches along SiC steps are well shorter than the Hall bar channel width. This explains the perfect quantization of the measured Hall resistances. On the other hand, series of bilayer stripes extending along titled SiC edge steps, could lead to current constrictions and explain the reduction of the width over which the Hall voltage drops (which also corresponds to the effective current channel width) although they only represent about 10% of the surface. Another explanation could be the existence of short-scale inhomogeneities of the carrier density in the sample although Hall resistance measurements, performed at different places in the Hall bar, do not reveal large carrier density fluctuations (less than 10%). Such inhomogeneities of the carrier density are indeed known to constrain the current circulation and to reduce the breakdown current density of the QHE[13].

The 2D color plot of fig. 2 gives a direct visualization of $I(B)$ curves at constant longitudinal resistance

value. They are sub-linear, as highlighted by the black line which gives the evolution of the threshold current I_C (which can be used to define a breakdown current of the QHE) above which $R_{xx} > 0.25 \text{ m}\Omega$. $I_C(B)$ continuously increases from $40 \text{ }\mu\text{A}$ to $60 \text{ }\mu\text{A}$ for B varying from 10 T to 19 T. This corresponds to breakdown current densities varying from 0.4 A/m to 0.6 A/m . These values are similar to those measured in GaAs based QHRS but well below the best values reported in graphene grown by Si sublimation from SiC[36]. On the other hand, if we consider the effective width $W_{eff} = 7.5 \text{ }\mu\text{m}$ and the $I_C(B)$ values determined, we calculate higher breakdown current densities of 5.5 A/m at 10 T, 6.7 A/m at 14 T, and 8 A/m at 19 T, in agreement with values expected in graphene. The sub-linear evolution of I_C as a function of B can also be explained by the VRH mechanism. Given that $\sigma_{xx} \propto \exp[(-I_0/I)^{1/2}]$, we indeed expect a sharp increase of conductivity for $I_C \sim I_0$ with $I_0 \propto \xi^{-2}$ (at this critical current the tiny variation of σ_0 becomes negligible). Fig. 2 indeed shows that $\xi^{-2}(B)$ (red dots) well adjusts to the $I_C(B)$ (black line).

Discussion about the B -width of the $R_K/2$ Hall resistance plateau. In graphene, the combination of a large energy gap, the existence of LL at zero energy and a moderate carrier mobility, which ensures a large mobility gap are favorable to a wide extension of the $R_K/2$ Hall resistance plateau, well beyond the magnetic field corresponding to $\nu_{n0} = 2$. Such wide and asymmetric (with respect to the magnetic field giving $\nu_{n0} = 2$) $R_K/2$ Hall resistance plateaus have even been reported in some works either in exfoliated graphene[37] or in epitaxial graphene grown on the C-terminated face of SiC [38]. Their quantization properties were characterized by a minimum of the longitudinal resistance occurring at a magnetic field corresponding to $\nu_{n0} = 2$. It results that an increase of the dissipation level, for example caused by an increase of the measurement current, tends to restore a symmetric shape of both the Hall and the longitudinal resistance with respect to the magnetic field giving $\nu_{n0} = 2$.

In the sample considered in this work, the magnetic field extension of the $R_K/2$ Hall resistance plateau should correspond to a range of LL filling factor from $\nu_{n0} = 2.65$ ($B=5 \text{ T}$) down to $\nu_{n0} = 0.70$ ($B=19 \text{ T}$) if a carrier density n_0 constant with magnetic field is assumed. Moreover, the $\nu = 2$ and $\nu = 1$ LL filling factors should occur at $B=6.6 \text{ T}$ and $B=13.2 \text{ T}$ respectively. Measurements of R_{xx} at a low current value ($1 \text{ }\mu\text{A}$) as a function of B , reported in fig. 6a) reveals the existence of a tiny minimum which occurs at about $B=15 \text{ T}$ independently of the temperature between 1.3 K and 40 K, but not at $B=6.6 \text{ T}$, as would be expected in the hypothesis of a constant carrier density. On the other hand, $\nu = 2$ at $B=15 \text{ T}$ would mean a carrier density reaching $7.3 \times 10^{11} \text{ cm}^{-2}$ instead of $n_0 = 3.2 \times 10^{11} \text{ cm}^{-2}$. Moreover, this minimum is no more observable at larger currents of some tens of μA (see fig. 1-c) and fig. 2) while the increase of the dissipation

should, in principle, reinforce its existence. This behavior is not in agreement with observations reported in previously discussed works ref.[37, 38]. On the other hand, Tzalenchuk and co-workers[22] observed, in epitaxial graphene grown on the Si-terminated face of SiC, an asymmetric $R_K/2$ Hall resistance plateau extending towards large magnetic fields that stays robust when increasing the dissipation. It was notably characterized by a continuous increase of the breakdown current of the QHE well beyond the magnetic field corresponding to $\nu_{n0} = 2$, as it is also observed in our sample (see fig. 5-a)). This was explained by a pinning of the LL filling factor at $\nu = 2$ caused by a charge transfer from the zero layer graphene (ZLG), specific to the growth on the Si-face of SiC, existing at the interface between the graphene and the substrate[39].

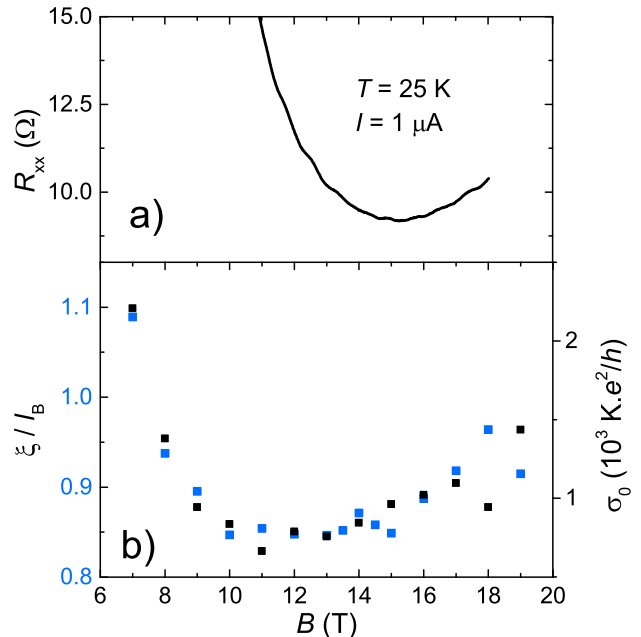


FIG. 6. a) R_{xx} versus B at $T=25 \text{ K}$ and $I = 1 \text{ }\mu\text{A}$. b) ξ/l_B (blue square) and σ_0 (black square) extracted from the VRH analysis as a function of the magnetic field B .

To deepen our understanding, $\xi(B)$, reported in fig. 4-b), was normalized by the magnetic length $l_B(B) = \sqrt{\hbar/eB}$ which describes the wavefunction characteristic size in the QHE regime. Fig. 6-b) shows that $\xi(B)/l_B(B)$ goes down when increasing B up to 10 T, stays almost constant at a minimal value close to one between $B=10 \text{ T}$ and $B=15 \text{ T}$, and then slowly increases at higher magnetic field. Let us remark that the determination of $\xi(B)$ values slightly lower than the magnetic length, not expected, is very likely related to the assumptions regarding the values of the dielectric constants of SiC (the presence of the ZLG on SiC is not taken into account) and of P(MMA-MAA) ($\epsilon_{P(MMA-MAA)}$ could be slightly different from $\epsilon_{P(MMA)}$), as well as of the C proportionality factor in the VRH expression of the conductivity

(for instance, a larger value $C = 7.4$ leads to $\xi(B) \geq l_B$ and might result from the partial inhomogeneity of our two-dimensional system caused by the presence of bilayer patches). In the magnetic field range from 10 T to 19 T, where the Hall resistance is perfectly quantized with a relative uncertainty of 10^{-9} , $\xi(B)$ remarkably stays very close, within about 10%, to $l_B(B)$ which is the minimal possible value for the localization length. Fig. 6-b) also shows that the dependence of $\sigma_0(B)$ and $\xi(B)/l_B(B)$ on B are similar. It appears that the minimum of R_{xx} , observed in fig. 6-a) at about $B=15$ T, occurs at the highest magnetic field where both $\sigma_0(B)$ and $\xi(B)/l_B(B)$ have the lowest values.

In the QHE regime, the localization length ξ is expected to vary according to $\xi \propto \xi_0/\nu^\gamma$ (with $\gamma \sim 2.3$ [40] and ξ_0 a length depending on the disorder potential) for $\nu \leq 2$ and approaching $\nu = 0$. In samples made of exfoliated graphene, this law was observed[41] to hold for ν values as high as 1.5. A lower bound value of ξ_0 is l_B , as predicted in case of short range disorder[42]). We therefore expect $\xi(B)/l_B(B)$ higher than $1/\nu(B)^\gamma$ which increases for decreasing ν values and then diverges at $\nu = 0$. For B varying from 10 T to 15 T, although $\nu_{n0}(B)$ decreases from 1.3 down to 0.9, $\xi(B)/l_B(B)$ is observed to stay constant. This is a first indication that $\nu(B)$ might stay close to $\nu = 2$. Away from the LL center near integer filling factors, it was proposed that $\xi(B)$ should approach the classical cyclotron radius[43]. A localization length approaching $r_c = \hbar k_F/eB$ at integer LL filling factor, where k_F is the Fermi momentum, was indeed observed in GaAs-based 2DEG[30]. In graphene, $r_c(B)$ can be written $r_c(B) = l_B(B)\sqrt{\nu/2}$ (since $k_F = \sqrt{\pi n_S}$). $r_c(B)$ is therefore proportional to $l_B(B)$ if $\nu(B)$ is constant (remarkably, one finds $l_B(B)$ for $\nu = 2$). The observation of $\xi(B) \sim l_B(B)$ therefore constitutes another argument suggesting that $\nu(B)$ could be pinned at $\nu = 2$ from 10 T to 15 T, and then decreases slowly up towards 19 T.

As discussed in Methods, structural characterizations by low energy electron diffraction shows the existence of a $(6R\sqrt{3} \times 6R\sqrt{3} - R30^\circ)$ reconstructed carbon-rich interface (ZLG) in our device[20]. Its presence explains the measured high n-doping ($10^{13}cm^{-2}$) of the pristine graphene layer (see methods). The low carrier density, determined at low magnetic fields, was obtained only after annealing and covering the sample with the P(MMA-MAA)/ZEP520A resist (not illuminated), as previously described. Thus, a transfer of charge from the ZLG leading to a pinning of $\nu(B)$ at $\nu \sim 2$ is possible and could explain the large width of the observed Hall resistance plateau, the absence of minima for both the localization length and the longitudinal conductivity at $B=6.6$ T. Using equations in ref.[22, 39] derived from the balance equation $\gamma[A - (e^2d/\epsilon_0)(n_S + n_g) - \epsilon_F] = n_S + n_g$ describing the charge transfer, it is possible to reproduce a pinning at $\nu = 2$ from $B=5.3$ T up to $B=15.1$ T with a zero magnetic field carrier density of $3.2 \times 10^{11}cm^{-2}$, considering $A=0.4$ eV, $d=0.3$ nm, $\gamma = 5.2 \times 10^{11}cm^{-2}(eV)^{-1}$ and $n_g = 1.55 \times 10^{12}cm^{-2}$, where A is the working func-

tion energy of the ZLG, d is the distance of the graphene layer to the ZLG, γ the density of donor states, and n_g the density of carriers transferred to the electrochemical gate. This is rather consistent with the experimental observations except that the analysis of the dependence of ξ/l_B on B rather indicates that the pinning of the filling factor should be effective at a higher magnetic field ($B=10$ T). Further experimental and theoretical works are needed to better understand the peculiarities of the charge transfer in graphene grown by propane/hydrogen CVD on SiC. Thereupon, the reduced effective width W_{eff} over which the Hall potential drops, as determined from the analysis of the dissipation, could be an indication of some degree of inhomogeneity of the charge transfer.

Conclusion. In a sample made of graphene grown by propane/hydrogen CVD on SiC, we report on the agreement of the quantum Hall resistance, measured on the $\nu = 2$ plateau in a 9 T range starting from 10 T at $T=1.4$ K, with $R_K/2$ within a relative uncertainty of 10^{-9} . Moreover, the relative discrepancy between the quantized Hall resistances in the graphene sample and in a reference GaAs one is equal to $(-2 \pm 4) \times 10^{-10}$. This constitutes a new proof of the universality of the QHE. The QHE physics of the wide quantized Hall resistance plateau is investigated using accurate specialized measurement techniques based on SQUID technology. From the characterization of the low dissipation, which is dominated by VRH, we determine that the localization length of states at Fermi energy stays locked to the magnetic field in the wide range of magnetic field where the Hall resistance is perfectly quantized. This can be explained by the pinning of the LL filling factor at $\nu = 2$ caused by a charge transfer from the buffer layer (ZLG) at the interface between the graphene and the SiC. The analysis of the dissipation also gives an effective width over which the Hall potential drops in the QHE regime which is probably linked to the graphene homogeneity (presence of bilayers patches or inhomogeneity of the carrier density).

To conclude, our work demonstrates, for the first time, that a graphene-based QHRS can substitute for its GaAs counterpart under the magnetic fields and low temperatures available in most national metrology institutes. This constitutes an essential step towards a resistance metrology based on low magnetic field and transportable graphene-based QHRS in the near future. Given that the propane/hydrogen CVD on SiC is a scalable growth technique that produces high quality graphene meeting the demanding requirements of the resistance metrology, it is likely that it will be suitable for other electronic applications of graphene as well.

Methods

Graphene growth. Graphene was grown by propane/hydrogen chemical vapor deposition (CVD)[19,

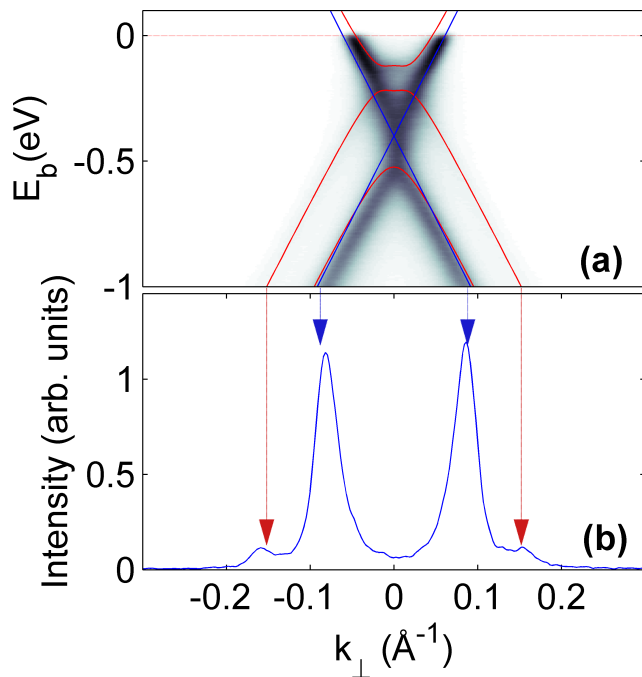


FIG. 7. a) ARPES spectra taken at the \bar{K} point of the graphene Brillouin zone for the sample after outgassing at 500°C . Spectra were acquired along the direction k_\perp perpendicular to the $\Gamma - \bar{K}$ direction in reciprocal space. The photon energy was 36 eV. The light was p polarized. The blue and solid lines are fits for monolayer and bilayer graphene respectively. b) Arpes intensity taken at $E_b = -1\text{eV}$, along k_\perp , evidences the small bilayer contribution at $k_\perp = \pm 0.17 \text{ \AA}^{-1}$. From the relative integrated intensity of the peaks attributed to mono and bilayer graphene, the coverage of the surface by bilayers can be estimated to be around 10 %.

21, 44] on the Si-face of a semi-insulating 0.16° off-axis 6H-SiC substrate from TankeBlue. We used a horizontal hot-wall CVD reactor with a hydrogen/argon mixture as the carrier gas at a pressure of 800 mbar. The graphene growth was obtained by adding a 5 sccm propane flow for 5 min at a growth temperature of 1550°C . Before the lithography, the graphene was extensively analyzed (sample HT-MLG in ref. [20]). Briefly, SiC steps of width 200 nm and height 0.75 nm were evidenced by AFM. Angle-resolved photoemission spectroscopy (ARPES) shows that a graphene monolayer covers the whole SiC surface but approximately 10 % is covered by patches of a second graphene layer (see fig. 7), mainly located along SiC edge steps as revealed by AFM. ARPES spectra also evidences high n-doping (10^{13}cm^{-2}) of the graphene monolayer, whose origin is linked to the presence of a $(6R\sqrt{3} \times 6R\sqrt{3} - R30^\circ)$ reconstructed carbon-rich interface detected by low-energy electron diffraction (LEED). Finally, a remarkable homogeneity of the graphene film over distances of several millimeters was evidenced by Raman spectroscopy.

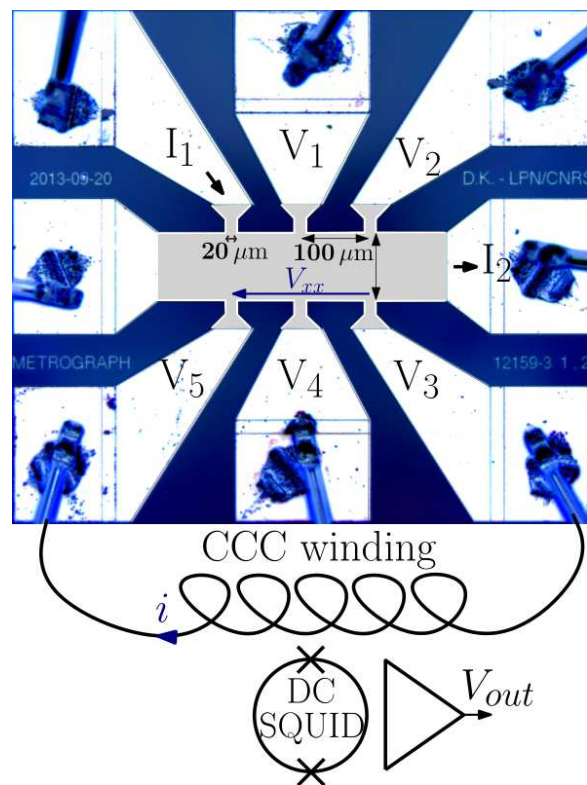


FIG. 8. Picture of Hall bar sample with characteristic lengths and terminal names. Schema of the measurement of V_{xx} using a winding of a CCC equipped with a DC SQUID.

Sample fabrication. The graphene sample was annealed in vacuum (a few times 10^{-4} torr pressure) for 1 min at 500°C (ramp of 500 s). The sample was left to cool down to below 100°C in vacuum over a few minutes. Subsequently, it was covered with polymethylmethacrylate (PMMA) for protection. The Hall bars were patterned using electron-beam lithography and PMMA resist. The graphene active areas were defined using oxygen reactive ion etching (RIE). Ohmic contacts to the graphene layer were formed by depositing a Pd/Au (60/20 nm) bilayer in an electron beam deposition system, using an ultrathin Ti layer for adhesion. Thicker Ti/Au (20/200 nm) bonding pads were formed in a subsequent step, where an RIE etch was performed prior to metal deposition for better adhesion of the metal pads to the SiC substrate. Finally the sample was covered for protection by 300 nm of poly(methylmethacrylate-co-methacrylate acid) copolymer (MMA (8.5) MAA EL10 from Microchem) and 300 nm of poly(methylstyrene-co-chloromethylacrylate) (ZEP520A from Zeon Chemicals) resist. The Hall bar has a width of $100 \mu\text{m}$ and a total length of $420 \mu\text{m}$. It has three pairs of Hall probes, separated by $100 \mu\text{m}$ (see fig. 8).

Measurement techniques. For all the reported measurements, the current circulates between I_1 and I_2

terminals. Longitudinal voltages are measured using terminal-pairs (V_1, V_2) and (V_3, V_5) . The longitudinal resistances indicated in the main text are normalized to a square. The Hall resistances are measured using terminal pairs (V_1, V_4) and (V_2, V_3) . The left terminal of the Hall bar has a resistance larger than 1Ω and is not used.

The Hall resistance R_H of a QHRS is compared to the 100Ω resistance of a transfer wire resistor using a resistance bridge based on a cryogenic current comparator (CCC). The CCC is a perfect transformer which can measure a current ratio in terms of the winding number of turns ratio with a relative uncertainty as low as a few 10^{-11} . Its accuracy relies on a flux density conservation property of the superconductive toroidal shield (Meissner effect), in which superconducting windings are embedded. Owing to a flux detector based on a DC superconducting quantum interference device (SQUID), the current noise resolution of the CCC is $80 \text{ pA.turn/Hz}^{1/2}$.

For measurements reported in fig. 1a), the resistance bridge operates in DC mode (the current is reversed every 28 s) and is equipped with a EMN11 nanovoltmeter as a null detector. The QHR and the 100Ω resistor are connected in series with a 2065 turns winding and a 16 turns winding respectively. R_{xx} is determined using an EMN11 nanovoltmeter to detect the longitudinal voltage V_{xx} resulting from the circulation of a DC current in the Hall bar.

For measurements reported in fig. 2 and fig. 5a)

and for two measurements reported in the text (Resistance quantization section) carried out at $B=10 \text{ T}$ and $B=19 \text{ T}$, the sample is biased with a DC current I and R_{xx} is measured using the CCC (see fig. 8). A 2065 turns winding of the CCC is connected to the two voltage terminals. The longitudinal voltage V_{xx} gives rise to the circulation of a current i in the winding of the CCC which is used as a current amplifier with a SQUID operating in internal feedback mode. The output of the SQUID electronics is measured with an Agilent 3458A multimeter. The current noise resolution is about $40 \text{ fA/Hz}^{1/2}$ which results in a voltage noise resolution of about $0.5 \text{ nV/Hz}^{1/2}$. The longitudinal resistance R_{xx} is then given by $R_{xx} = (i/I)R_H$ since the two-terminal impedance seen by the winding is very close to R_H on the $\nu = 2$ plateau.

For data reported in fig. 3 and fig. 4, quick and accurate measurements are carried out while the temperature of the sample is swept from 40 K down to 3 K . The Hall bar is then supplied with a AC (2 Hz frequency) current $I = 1 \mu\text{A}$, controlled by the reference voltage of a Signal Recovery 7265 lock-in detector. The Hall resistance R_H is measured using the resistance bridge replacing the EMN11 nanovoltmeter by a Celians EPC1 AC low-noise amplifier, whose output is connected to the lock-in detector. R_{xx} is measured using the same technique as in fig. 2 and fig. 5a), except that the output of the SQUID is connected to the lock-in detector.

References

- [1] K. V. Klitzing, Phys. Rev. Lett. **45**, 494 (1980).
- [2] F. Schopfer and W. Poirier, J. Appl. Phys. **114**, 064508 (2013).
- [3] W. Poirier, A. Bounouh, F. Piquemal, and J. P. André, Metrologia **41**, 285 (2004).
- [4] W. Poirier and F. Schopfer, Eur. Phys. J. Spec. Top. **172**, 207 (2009).
- [5] F. Schopfer and W. Poirier, MRS bulletin **37**, 1255 (2012).
- [6] K. S. Novoselov, A. K. Geim, S. V. Morozov, D. Jiang, M. I. Katsnelson, S. V. D. I. V. Grigorieva, and A. A. Firsov, Nature **438**, 197 (2005).
- [7] Y. B. Zhang, Y. W. Tan, H. Stormer, and P. Kim, Nature **438**, 201 (2005).
- [8] V. P. Gusynin and V. P. Sharapov, Phys. Rev. Lett. **95**, 146801 (2005).
- [9] K. S. Novoselov, Z. Jiang, Y. Zhang, S. V. Morozov, H. L. Stormer, U. Zeitler, J. C. Maan, G. S. Boebinger, P. Kim, and A. K. Geim, Science **315**, 1379 (2007).
- [10] W. Poirier and F. Schopfer, Nature Nanotechnology **5**, 171 (2010).
- [11] A. J. M. Giesbers, G. Rietveld, E. Houtzager, U. Zeitler, R. Yang, K. S. Novoselov, A. K. Geim, and J. C. Maan, Appl. Phys. Lett. **93**, 222109 (2009).
- [12] M. Woszczyna, M. Friedemann, M. Gotz, E. Pesel, K. Pierz, T. Weimann, and F. J. Ahlers, Appl. Phys. Lett. **100**, 164106 (2012).
- [13] J. Guignard, D. Leprat, D. C. Glatli, F. Schopfer, and W. Poirier, Phys. Rev. B **85**, 165420 (2012).
- [14] T. Shen, W. Wu, Q. Yu, C. A. Richter, R. Elmquist, D. Newell, and Y. P. Chen, Appl. Phys. Lett. **99**, 232110 (2011).
- [15] F. Lafont, R. Ribeiro, Z. Han, S. Roche, V. Bouchiat, F. Schopfer, and W. Poirier, arXiv:1404.2536 (2014).
- [16] A. Tzalenchuk, S. Lara-Avila, A. Kalaboukhov, S. Paolillo, M. S. Syvajarvi, R. Yakimova, O. Kazakova, T. J. B. M. Janssen, V. Falko, and S. Kubatkin, Nature Nanotechnology **5**, 186 (2010).
- [17] T. J. B. M. Janssen, N. Fletcher, R. Goebel, J. Williams, A. Tzalenchuk, R. Yakimova, S. Kubatkin, S. Lara-Avila, and V. Falko, New J. Phys. **13**, 093026 (2011).
- [18] A. Satrapinski, S. Novikov, and N. Lebedeva, Appl. Phys. Lett. **103**, 173509 (2013).
- [19] A. Michon, S. Vézian, A. Ouerghi, M. Zielinski, T. Chasagne, and M. Portail, Appl. Phys. Lett. **97**, 171909 (2010).
- [20] B. Jabakhanji, A. Michon, C. Consejo, W. Desrat, M. Portail, A. Tiberj, M. Paillet, A. Zahab, F. Cheymis, F. Lafont, F. Schopfer, W. Poirier, F. Bertran, P. L. Fvre, A. Taleb-Ibrahimi, D. Kazazis, W. Escoffier, B. C. Camargo, Y. Kopelevich, J. Camassel, and B. Jouault, Phys. Rev. B **89**, 085422 (2014).
- [21] A. Michon, L. Largeau, A. Tiberj, J.-R. Huntzinger,

- O. Mauguin, S. Vézian, D. Lefebvre, F. Cheynis, F. Leroy, P. Muller, T. Chassagne, M. Zielinski, and M. Portail, *Materials Science Forum* **740-742**, 117 (2013).
- [22] T. J. B. M. Janssen, A. Tzalenchuk, R. Yakimova, S. Kubatkin, S. Lara-Avila, S. Kopylov, and V. I. Falko, *Phys. Rev. B* **83**, 233402 (2011).
- [23] S. Lara-Avila, K. Moth-Poulsen, R. Yakimova, T. Bjornholm, V. Falko, A. Tzalenchuk, and S. Kubatkin, *Adv. Mater.* **23**, 878 (2011).
- [24] F. Piquemal, G. Genevès, F. Delahaye, J. P. André, J. N. Patillon, and P. Frijlink, *IEEE Trans. Instrum. Meas.* **42**, 264 (1993).
- [25] W. van der Wel, Ph.D. thesis, University of Delft (1988).
- [26] Dominguez, Ph.D. thesis, CNAM, Paris (1987).
- [27] W. van der Wel, C. J. P. M. Harmans, and J. E. Mooij, *J. Phys. C: Solid State Physics* **21**, L171 (1988).
- [28] B. I. Shklovskii and A. L. Efros, *Electronic properties of Doped semiconductors* (Springer, 1984).
- [29] N. V. Lien, *Sov. Phys. Semicond.* **18**, 207 (1984).
- [30] M. Furlan, *Phys. Rev. B* **57**, 14818 (1998).
- [31] L. Patrick and W. J. Choyke, *Phys. Rev. B* **2**, 2255 (1970).
- [32] B. Jeckelmann and B. Jeanneret, *Rep. Prog. Phys.* **64**, 1603 (2001).
- [33] C. Chua, M. Connolly, A. Lartsev, T. Yager, S. Lara-Avila, S. Kubatkin, S. Kopylov, V. Falko, R. Yakimova, R. Pearce, T. J. B. M. Janssen, A. Tzalenchuk, and C. G. Smith, *Nano Lett.* **14**, 3369 (2014).
- [34] T. Schumann, K.-J. Friedland, M. H. O. Jr., A. Tahraoui, J. M. J. Lopes, and H. Riechert, *Phys. Rev. B* **85**, 235402 (2012).
- [35] T. Lofwander, P. San-Jose, and E. Prada, *Phys. Rev. B* **87**, 205429 (2013).
- [36] J. A. Alexander-Webber, A. M. R. Baker, T. J. B. M. Janssen, A. Tzalenchuk, S. Lara-Avila, S. Kubatkin, R. Yakimova, B. A. Piot, D. K. Maude, and R. J. Nicholas, *Phys. Rev. Lett.* **111**, 096601 (2013).
- [37] J.-M. Pomirol, W. Escoffier, A. Kumar, B. Raquet, and M. Goiran, *Phys. Rev. B* **82**, 121401(R) (2010).
- [38] B. Jouault, N. Camara, B. Jabakhanji, A. Caboni, C. Consejo, P. Godignon, D. K. Maude, , and J. Camassel, *Appl. Phys. Lett.* **100**, 052102 (2012).
- [39] A. T. S. Kopylov, S. Kubatkin, and V. I. Falko, *Appl. Phys. Lett.* **97**, 112109 (2010).
- [40] D. Yoshioka, *The quantum Hall effect* (Springer, 1998).
- [41] K. Bennaceur, P. Jacques, F. Portier, P. Roche, and D. C. Glattli, *Phys. Rev. B* **86**, 085433 (2012).
- [42] D. G. Polyakov and B. I. Shklovskii, *Phys. Rev. Lett.* **70**, 3796 (1993).
- [43] M. M. Fogler, A. Y. Dobin, and B. I. Shklovskii, *Phys. Rev. B* **57**, 4614 (1998).
- [44] J. Hwang, V. B. shields, C. I. Thomas, S. Shivaraman, D. Hao, M. Kim, A. R. Woll, G. S. Tompa, and M. G. Spencer, *J. Cryst. Growth.* **312**, 3219 (2010).

Acknowledgments We wish to acknowledge D. Leprat for technical support and M. Paillet for advices about structural characterizations. This research has received funding from the french Agence Nationale de la Recherche (Metrograph project, Grant No. ANR-2011-NANO-004).

Author contributions W. P and F. S. planned the experiments. A. M. fabricated the graphene layer. A. M., T. C, M. Z and M. P developed the growth technology. D. K. fabricated the Hall bar. F. L., R. R-P., F. S., W. P. conducted the electrical measurements. B. J. performed ARPES measurements. D. K., B. J., C. C and O. C carried out complementary electrical measurements. F. L., R. R-P., F. S., W. P. analyzed the data. W. P., F. S, F. L, R. R-P, B. J, A. M, D. K wrote the paper with all authors contributing to the final version.